

MHD Nanofluid Flow with Slip conditions over an Inclined Non-linear Stretching Surface in Porous Media

Sham Bansal

Department of Mathematics, Mata Gujri College, Fatehgarh Sahib, Punjab, India

shambansal2010@gmail.com

ARTICLE INFO

Received: 24 Dec 2024

Revised: 18 Feb 2025

Accepted: 28 Feb 2025

ABSTRACT

This research analyses the behaviour of a magnetohydrodynamic nanofluid flowing across an inclined surface that stretched in a non-linear fashion. The fluid's motion is constrained by a porous matrix, and interfacial phenomena are captured by thermal and velocity slip models. The study utilizes similarity variables to reduce the partial differential equations to a system of dimensionless ordinary differential equations. The numerical solution is achieved through the Keller-box technique. The analysis reveals the complex influence of various factors, including the thermal slip factor, stretching factor, permeability factor, thermophoresis, velocity slip factor, magnetic field strength and Brownian motion factor. The temperature and concentration along with velocity profiles inside the fluid domain are substantially impacted by these factors. The findings indicate that higher inclination angles enhance both concentration and temperature, while simultaneously diminishing the velocity profile. An increase in permeability enhances fluid mobility by lowering flow resistance, leading to higher thermal conductivity. Both concentration and temperature trajectories demonstrate a pronounced upward trend with increasing magnetic field strength, while fluid velocity experiences a decline. Furthermore, a higher velocity slip value leads to a rise in the heat transmission rate, while skin friction and the rate of mass transport experiences a decrease.

Keywords: Magnetohydrodynamics, Nanofluid, Stretching sheet, Porous Medium.

1. Introduction

Real-world scenarios often involve slip conditions develop at the fluid-solid interface. Thermal wall slip arises due to a temperature discontinuity at the boundary, while velocity slip signifies a discrepancy between the fluid's velocity near the wall and the wall's own velocity. These factors significantly influence the performance and efficiency of nanofluid-based systems. Understanding the impacts of such slip effects is vital for boosting the efficiency of engineering systems, enhancing heat transfer efficiency, and developing innovative applications in domains that include microfluidics, nanotechnology and cooling electronics. (Jamrus et al., 2024) investigates the influence of slip conditions on the magnetohydrodynamic mixed convective transport of nanofluids across a stretching surface. The study emphasizes the role of velocity slip in modulating the fluid movement and transfer of heat attributes, offering insights into the optimization of thermal management systems. (Guled et al., 2024) explores the joint impact of thermal wall slip and slip velocity on the Magnetohydrodynamics (MHD) flow of nanofluids across a stretching sheet. The findings highlight the importance of slip conditions in enhancing the efficiency of mass and heat transport mechanisms in engineering applications. (Abbas et al., 2023) analyse the impact of thermal slip in modulating nanofluid flow and heat transport across a porous extensible or shrinking surface. Their findings offer key data for

improving nanofluid-driven thermal systems. (Yin et al., 2019) examines the effects of ion slip on the entropy formation in rotating nanofluid flow across an infinite plate. The research underscores the significance of slip conditions in minimizing entropy generation and enhancing the thermodynamic functioning of fluid systems. (Hayat et al., 2016) investigate the simultaneous effects of slips on the heat transfer across a surface that stretches exponentially. The study's findings are pertinent for designing improved heat management solutions across numerous engineering sectors.

The study of MHD boundary layer flow involving nanofluids has garnered significant focus nowadays for its extensive usages in engineering and industrial processes. MHD explores the behaviour of electrically conducting fluids in the presence of a magnetic factor, merging principles from both fluid dynamics and electromagnetism. The study of MHD effects on fluid dynamics and heat transport is crucial for an array of applications, involving cooling systems for nuclear reactors, magnetic drug targeting, metallurgical processes, and astrophysical phenomena. Understanding how magnetic fields influence fluid flow and heat transfer enables engineers and scientists to produce systems with improved efficiency and inventive solutions to complex problems in various industries. (Reddy et al., 2023) investigates the cumulative impact of radiation, heat source, and MHD within the flow of a viscoelastic liquid across a stretched surface. The results highlight the role of magnetic fields on enhancing heat transmission in viscoelastic fluids. (Kumar et al., 2022) researched the buoyancy-driven flow of a MHD nanofluid across a stretched surface, considering the effects of heat generation and thermal radiation. The findings provide valuable perspectives for enhancing heat exchange efficiency in engineering systems that utilize nanofluids and magnetic fields. (Goud et al., 2023) investigates the magnetic field significance on mixed convection heat transmission Maxwell flow across vertical plate, accounting for viscous dissipation effect. The results contribute to the advancement of higher-efficiency cooling systems in the nuclear industry and other high-temperature applications. (Bulatova et al., 2020) investigates the flow behaviour around a body in a magnetic field. The fluid is electrically conductive, viscous, and exhibits a non-linear interaction among strain and stress. (Sudarmozhi et al., 2024) explores the viscoelastic flow impacted by radiation and magnetic forces, focusing on the synergistic impacts on fluid behaviour and heat transport. The findings are pertinent to applications where both magnetic fields and radiation play a significant role.

Nanofluids, which are formed by suspending nanoparticles within a base fluid, yields superior thermal capabilities than conventional fluids. These enhanced properties make nanofluids ideal for applications in heat transfer, lubrication, and cooling systems. When exposed to an exogenous magnetic force, the behaviour of nanofluids can be significantly altered, affecting the flow and heat transport capabilities. The introduction of nanoparticles considerably improves the conductive ability of the base fluid, making nanofluids highly appropriate for an array of applications, from cooling systems in electronics to advanced heat exchangers. (Kakac et al., 2009) reviews the nanofluids' ability to strengthen convective heat transport. The study discusses various mechanisms through which nanoparticles improve heat transmission rates, and examines the emerging benefits of nanofluids in different thermal systems. (Hyder et al., 2024) researched the heat transmission attributes of nanofluids, focusing on their capability for superior thermal output in numerous of applications. (Ouada et al., 2023) explores convective heat exchange in hybrid nanofluids via a moving porous fin, emphasizing the affect of nanoparticles dispersion on heat transmission rates and convection currents. (Seid et al., 2022) researched the importance of multiple slip mechanisms and Soret effect on the boundary layer behaviour of an electrically conductive nanofluid travelling across a vertically stretched surface.

Porous media are essential to the operation in various natural and engineered systems, significantly impacting fluid dynamics. An extensive understanding of porous structures is indispensable to effectively refine processes across geothermal energy, petroleum extraction, chemical reaction systems, and environmental remediation. The bonding among the nanofluid and the porous matrix influences flow resistance, heat conduction, and mass transfer, making it a complex yet vital area

of study. Research in this domain seeks to elucidate the mechanisms governing fluid movement and thermal transport through porous media, providing insights that enhance the efficiency and effectiveness of these systems. (Kaviany et al., 2012) provides a thorough examination of heat transfer principles within porous media, offering both theoretical observations and practical applications. This is a beneficial source for scholars and engineers working with porous structures. (Chernukha et al., 2024) develops a mathematical model describing the transport of impurity particles within a three-layered porous material. This model considers both convective diffusions, where the particles are carried by a flowing fluid, and sorption processes, where the particles interact with the porous material itself. (Zhang et al. 2021) analyses the Forchheimer flow and heat transport capabilities embedded in a channel, providing foundational capabilities into the complex interplay among fluid flow and porous structures. (Bansal et al., 2024) investigated how nanofluids and magnetic fields can work together to improve heat transfer efficiency in porous materials.

The finite difference Keller-box implicit (FDKBI) method is a robust computational technique widely used in tackling partial differential equations (PDEs) that arise in heat transfer studies. This method is known for its stability and accuracy in handling boundary layer problems, complex geometries, and nonlinear equations. The FDKBI scheme discretizes the governing equations into a finite difference form, allowing for the efficient computation of numerical solutions. Its implicit nature ensures convergence and stability, making it an ideal choice for simulating fluid flow and heat transmission in various engineering systems. Studies by (Gupta, 2015; Smith, 1985) demonstrate the advantages of implicit methods for achieving high-accuracy solutions to PDEs. (Sarif et al., 2013; Rafique et al., 2024) applied the FDKBI method to unsteady MHD flow and heat transmission of nanofluids across a stretched surface. It highlights the method's robustness in dealing with time-dependent problems and its applicability to nanofluid dynamics. (Ramya et al., 2018) employed the FDKBI approach to study MHD flow of a nanofluid via a non-linear stretching surface. The study showcases the method's capability handling nonlinearities and complicated boundary conditions in heat transfer problems. (Ishak et al., 2009) employed the FDKBI approach for evaluating MHD stagnation-point flow and heat transmission, considering imposed magnetic fields and thermal radiation. It emphasizes the method's versatility in solving various MHD and heat transfer problems.

Despite extensive research on MHD nanofluid flow, the effects of thermal and velocity slip at boundaries have yet to be extensively studied. This research seeks to address the gap by offering new insights into practical applications and endeavours to shed light on the combined effects of velocity and thermal slips on the nanofluids MHD boundary layer flow across a non-linearly inclined stretched surface via a porous medium. These factors are critical as they significantly impact flow dynamics and heat transmission characteristics, presenting opportunities to enhance efficiency in various engineering applications. By researching these aspects, we intend to acquire a better understanding of the core physics and develop strategies to enhance the performance of systems that utilize nanofluids in MHD applications. The situation gets even more intricate in non-Darcy flows, where the resistance experienced by the flow through a porous media deviate from the traditional linear Darcy law. The insights gleaned from this study are expected to pave the way for advancements in technologies across diverse fields.

2. Mathematical Formulation

This research explores the complex interactions among thermal slip, velocity slip and MHD affects on structural features of boundary layer. The study addresses a steady, incompressible flow of a nanofluid in two dimensions. In order to preserve laminar flow within the boundary layer, the Reynolds number is maintained at a low value. The porous media is supposed to be homogeneous and isotropic, with consistent porosity and permeability. The interface separating the nanofluid and the inclined stretched surface, there is a non-zero velocity slip, determined as a slip factor that dictates the extent of the velocity slip. Additionally, a temperature difference, though limited, occurs across this boundary and

this jump is represented by the length of thermal slip, accounts for the temperature difference between the nanofluid and the stretched sheet. The imposed magnetic field varies spatially, enabling the study concerning its varying affect on the fluid. The stretching surface’s velocity adheres to a non-linearly relation, given by $u_w = ax^n$, with n indicates the stretching factor and a denotes the stretching rate. This enables for the analysis of alternative stretching possibilities besides the linear case. The sheet’s temperature (T_w) is consistent throughout. The fluid’s temperature distant from the stretched surface is consistently maintained at (T_∞). The sheet also exhibits a uniform concentration (C_w) of nanoparticles and a constant concentration (C_∞) across the fluid distant from the stretched surface. Figure 1 depicts visual representation of the physical features of the current study. Mathematical formulations and accompanying boundary restrictions for this problem have been presented by ([23], [25], [26]). The subsequent analysis of nanofluid flow is described by the following four interrelated equations:

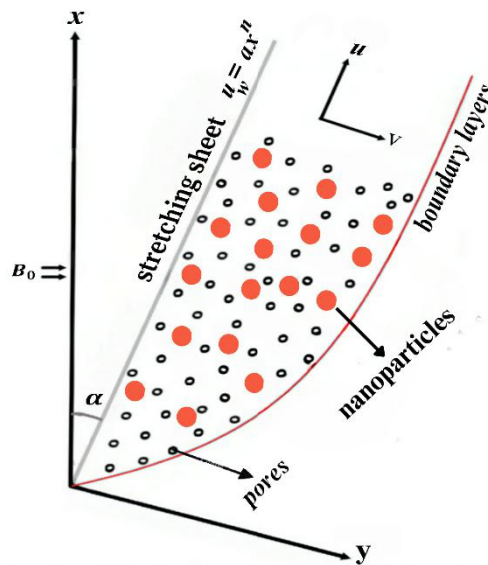


Figure 1 Physical Setup for the current research problem

$$\frac{\partial u}{\partial x} + \frac{\partial v}{\partial y} = 0 \tag{1}$$

$$u \frac{\partial u}{\partial x} + v \frac{\partial u}{\partial y} = \frac{\mu_{nf}}{\rho_{nf}} \frac{\partial^2 u}{\partial y^2} + [g\beta_T(T - T_\infty) + g\beta_C(C - C_\infty)]\text{Cos}(\alpha) - \frac{\sigma(B(x))^2}{\rho_{nf}} u - \frac{\mu_{nf}}{\rho_{nf} K_d} u \tag{2}$$

$$u \frac{\partial T}{\partial x} + v \frac{\partial T}{\partial y} = \frac{\mu_{nf}}{(\rho C_p)_{nf}} \left(\frac{\partial u}{\partial y}\right)^2 + \alpha_{nf} \frac{\partial^2 T}{\partial y^2} + \tau [D_m \frac{\partial T}{\partial y} \frac{\partial C}{\partial y} + \frac{D_r}{D_\infty} \left(\frac{\partial T}{\partial y}\right)^2] \tag{3}$$

$$u \frac{\partial C}{\partial x} + v \frac{\partial C}{\partial y} = D_m \frac{\partial^2 C}{\partial y^2} + \frac{D_r}{T_\infty} \frac{\partial^2 T}{\partial y^2} \tag{4}$$

Considering a variable magnetic field defined by $B(x) = B_0 x^{\frac{n-1}{2}}$ and utilizing the following properties for nano-fluids:

Thermal diffusivity $\alpha_{nf} = \frac{\kappa_{nf}}{(\rho C_p)_{nf}}$, effective viscosity $\mu_{nf} = \frac{\mu_f}{(1-\phi)^{2.5}}$ and effective heat capacity ratio $\tau = \frac{(\rho C_p)_s}{(\rho C_p)_f}$, the last term in equation (2) accounts for non-Darcy flow effects. β_C and β_T are concentration and thermal expansion coefficients respectively and α is inclination angle.

$$C = C_w, u = u_w + N v_f \frac{\partial u}{\partial y} = ax^n + N_0 x^{-\frac{n+1}{2}} v_f \frac{\partial u}{\partial y}$$

$$v = 0 \text{ \& } T = T_w + D \frac{\partial T}{\partial y} = T_\infty + ax^{2n} + D_0 x^{-\frac{n+1}{2}} \text{ at } y = 0$$

$$\text{and } u \rightarrow 0, v \rightarrow 0, T \rightarrow T_\infty, C \rightarrow C_\infty \text{ if } y \rightarrow \infty \tag{5}$$

Equation (5) outlines boundary conditions that delineate the behaviour of velocity and thermal slips near the stretching sheet. Specifically, the velocity slip, denoted as N , is expressed as $N_0 x^{-\frac{n+1}{2}}$, while the thermal slip, D , is represented by $D_0 x^{-\frac{n+1}{2}}$. Here, N_0 and D_0 correspond to the initial values of velocity and thermal slips, respectively, and n is the stretching factor. Moreover, the sheet temperature T_w is determined by $T_\infty + ax^{2n}$, and the stretching velocity u_w is given by ax^n , with ‘ a ’ signifying the stretching rate.

Similarity transformations can be characterized as:

$$\theta(\eta) = \frac{T-T_\infty}{T_w-T_\infty}, v = -x^{-\frac{n+1}{2}} \left[\frac{a(n+1)v_f}{2} \right]^{\frac{1}{2}} [f(\eta) + \eta \frac{n-1}{n+1} f'(\eta)],$$

$$\eta = yx^{-\frac{n+1}{2}} \left(\frac{a(n+1)}{2v_f} \right)^{\frac{1}{2}}, u = ax^n f'(\eta) \text{ and } \xi(\eta) = \frac{C-C_\infty}{C_w-C_\infty} \tag{6}$$

Presenting a stream function, represented by $\psi(x, y)$, which is characterized by its adherence to equation (1), expressed as:

$$u = \frac{\partial \psi}{\partial y} \text{ \& } v = -\frac{\partial \psi}{\partial x} \tag{7}$$

The equations (2-4), when transformed using equations (6-7), yield the following set of non-dimensional ODEs:

$$f'''(\eta) + f''(\eta)f(\eta) - [Gr_x \theta(\eta) + Gr_x \xi(\eta)] \cos(\alpha) - \frac{2n}{n+1} (f'(\eta))^2 - f'(\eta)(M + K) = 0 \tag{8}$$

$$[\xi'(\eta)N_b + f(\eta)]\theta'(\eta) - \frac{4n}{n+1} \theta(\eta)f'(\eta) + (\theta'(\eta))^2 N_t + (f''(\eta))^2 Ec = 0 \tag{9}$$

$$\xi''(\eta) + \frac{N_t}{N_b} \theta''(\eta) - \xi'(\eta)f(\eta)Le = 0 \tag{10}$$

Utilizing the relationship defined in equation (6), the boundary restrictions described in equation (5) are transformed to:

$$\theta(\eta) = 1 + \beta \theta'(0), \xi(\eta) = 1, f'(\eta) = 1 + \lambda f''(0), f(\eta) = 0 \text{ for } \eta = 0$$

$$\text{and } \xi(\eta) \rightarrow 0, f'(\eta) \rightarrow 0, \theta(\eta) \rightarrow 0 \text{ when } \eta \rightarrow \infty \tag{11}$$

The parameters are configured as follows:

$$N_b = \frac{(\rho c)_s D_m (C_w - C_\infty)}{v_f (\rho c)_f}, Gr_x = \frac{g \beta_C (C_w - C_\infty)}{a^2 x}, N_t = \frac{D_r (\rho c)_s (T_w - T_\infty)}{v_f T_\infty (\rho c)_f},$$

$$\beta = D_0 \left(\frac{a(n+1)}{2v_f} \right)^{\frac{1}{2}}, K = \frac{2v_f}{a(n+1)K_d}, Pr = \frac{v_f}{\alpha_f}, \lambda = N_0 \left(\frac{av_f(n+1)}{2} \right)^{\frac{1}{2}},$$

$$M = \frac{2\sigma B_0^2}{a(n+1)\rho_f}, Ec = \frac{x^{2n} a^2}{(T_w - T_\infty)(c_p)_f}, Gr_x = \frac{g \beta_T (T_w - T_\infty)}{a^2 x}, Le = \frac{\alpha_f}{D_m} \tag{12}$$

In present analysis, the primary physical measures under consideration are the mass transfer rate ($-\xi'(0)$), skin friction coefficient ($f''(0)$) and heat transmission rate ($-\theta'(0)$). These are mathematically represented by:

$$-\xi'(0) = Sh \left(\frac{2}{n+1} Re_x\right)^{1/2}, f''(0) = C_f \left(\frac{2}{n+1} Re_x\right)^{1/2}$$

$$\text{and } -\theta'(0) = Nu \frac{\kappa_f}{\kappa_{nf}} \left(\frac{n+1}{2} Re_x\right)^{-1/2} \tag{13}$$

where, $Sh = \frac{-xq_m}{D_m(C_\infty - C_w)}$ is Sherwood number that quantifies the convective mass transfer, $Re_x = \frac{xu_w}{\nu}$ is local Reynolds number that characterizes the flow regime, $C_f = \frac{\tau_w}{\rho_f u_w^2}$ is skin friction, which depicts the shear stress acting on the surface and $Nu = \frac{-xq_w}{\kappa_f(T_\infty - T_w)}$ represents Nusselt number that signifies the convective heat transfer.

3. Results and Discussion

This research explores the behaviour of magnetohydrodynamic nanofluid flow across an inclined non-linearly stretching sheet embedded in a porous matrix, considering the affects of slip velocity and thermal slip. By examining the complex interplay of parameters such as the Brownian motion factor (N_b), magnetic factor (M), velocity slip (λ), stretching factor (n), thermophoresis factor (N_t), permeability factor (K), inclination angle (α) and thermal slip (β) on the concentration ($\xi(\eta)$), velocity ($f'(\eta)$) and temperature ($\theta(\eta)$) profiles, as well as the boundary layer structures, this study provides valuable insights into intricate fluid dynamic phenomena. Understanding these influences is vital in predicting and controlling fluid behaviour in an array of industrial applications. The governing equations are computed numerically employing the FDKBI method, and the resulting solutions are expressed graphically. For numerical computations, the following default values for physical parameters were employed: $\alpha = 60^\circ$, $M = 0.5$, $Le = 5$, $Pr = 6.8$, $N_t = K = \lambda = Ec = N_b = 0.1$, $n = 2$ and $\beta = 0.2$, unless otherwise specified.

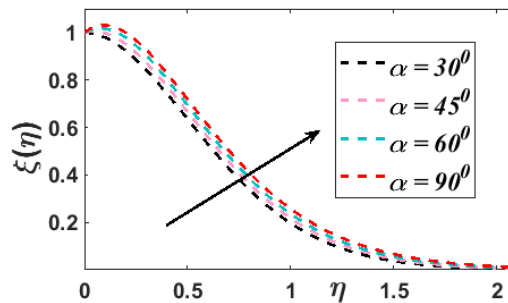


Figure 2 Impact of inclination angle α on Concentration

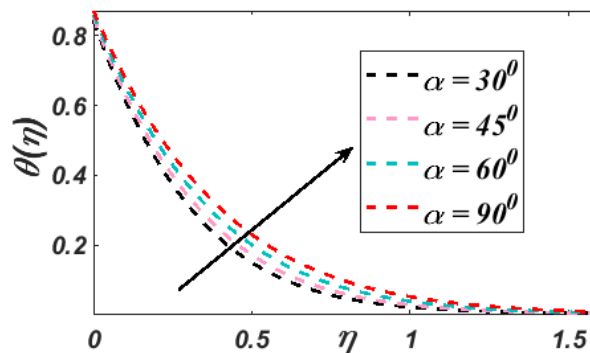


Figure 3 Impact of inclination angle α on Temperature

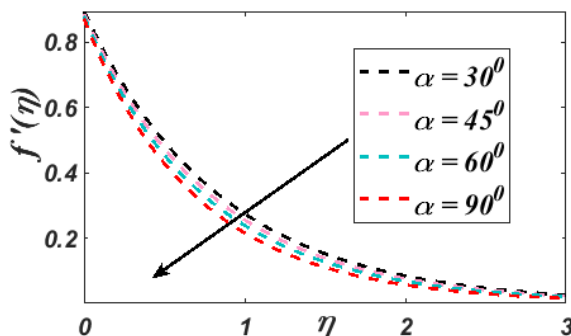


Figure 4 Impact of inclination angle α on velocity

Figure 2 illustrates the significance of the inclination angle α on the concentration $\xi(\eta)$. A rise in α leads to a hike in $\xi(\eta)$. A similar trend is observed for the temperature profile $\theta(\eta)$ illustrated in Figure 3. Conversely, the velocity profile $f'(\eta)$, as appeared in Figure 4, exhibits the opposite behavior, decreasing with a rise in the inclination angle. This behavior can be attributed to the influence of gravitational forces. At smaller inclination angles, the effect of gravity is more pronounced. As the inclination angle increases, the effect of buoyancy forces diminishes, causes a drop in the velocity profile.

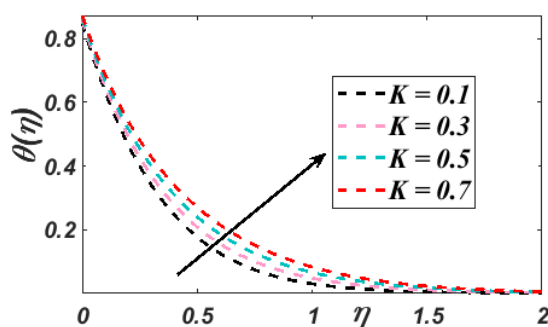


Figure 5 Impact of permeability parameter K on Temperature

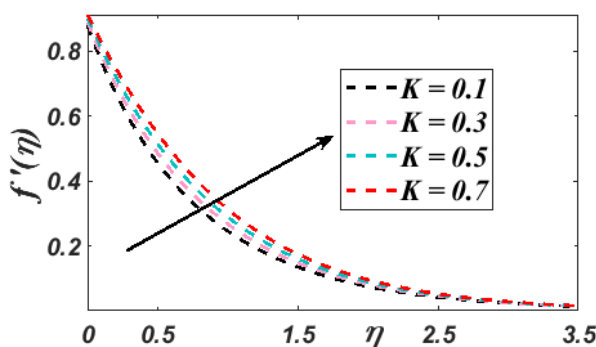


Figure 6 Impact of permeability parameter K on Velocity

The permeability parameter, K , has a substantial impact on the boundary layer properties and heat transmission within the system. A rise in K improves fluid mobility by lowering flow resistance to flow within the porous medium. This enhanced flow facilitates an enhanced thermal conductivity of the fluid, as evident in Figure 5. Concurrently, the reduced resistance allows the nanofluid to flow more freely, resulting in a thinner velocity boundary layer and greater fluid velocity, $f'(\eta)$, closer to the surface, as displayed in Figure 6. However, the effect of permeability on nanoparticle concentration,

$\xi(\eta)$, exhibits a more complex behavior. As shown in Figure 7, a hike in K initially leads to a reduction in $\xi(\eta)$ near the surface ($\eta = 0$) and then an increase further away from the surface ($\eta > 0.5$). This suggests that variations in permeability can significantly impact nanoparticle transport within the boundary layer, affecting both diffusive and convective mechanisms.

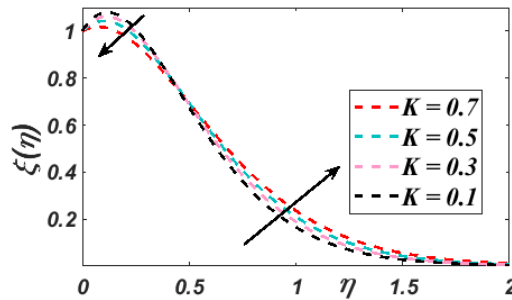


Figure 7 Impact of permeability parameter K on Concentration

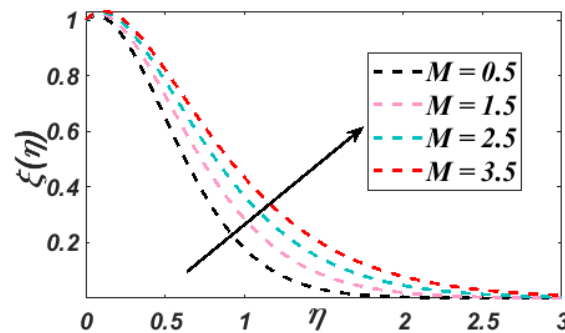


Figure 8 Impact of Magnetic parameter M on Concentration

The influence of the magnetic factor on the fluid flow enormously alters the boundary layer features. This parameter notably influences heat transmission rates. Figures (8–10) illustrate a substantial spike in both temperature and concentration trajectories with increasing magnetic field strength. This observation aligns with the well-established phenomenon of improved thermal conductivity in nanofluids containing metallic nanoparticles when exposed to a magnetic field. Conversely, a hike in the magnetic factor causes a decrease in the fluid velocity, $f'(\eta)$. This drop can be attributed to the appearance of the Lorentz force, a resistive force generated as an electrically conducting fluid comes into contact under a magnetic force. This contrary force enables to decelerate the fluid flow.

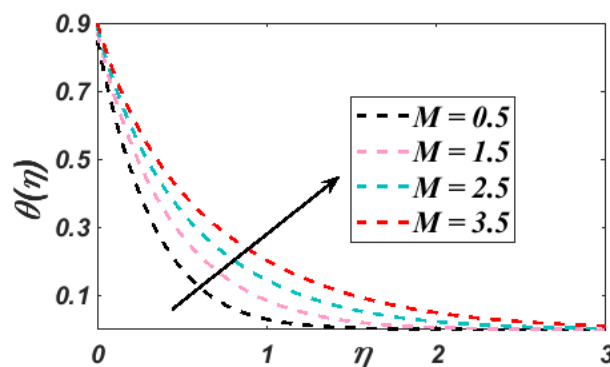


Figure 9 Impact of Magnetic parameter M on Temperature

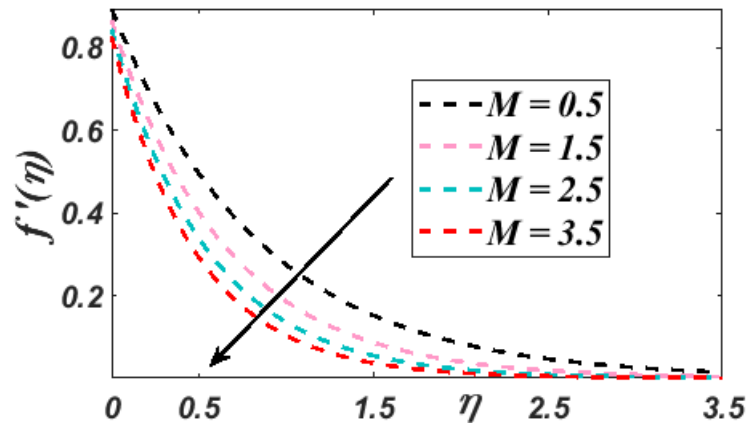


Figure 10 Impact of Magnetic parameter M on Velocity

The numerical results detailed in Table 1 summarizes the computational results for $-f''(0)$, $-\xi'(0)$ and $-\theta'(0)$ across numerous values of λ , α and β . These computations were carried out with consistent settings for parameters $Ec = K = 0.1$, $N_b = N_t = 0.3$, $Le = 5$, $Pr = 6.8$ and $M = n = 2$. A significant finding is that augmenting the thermal slip factor β lowers heat and mass transport. This downward tendency is related to less surface friction. The coefficient of skin friction is insensitive to changes in β . Moreover, rising the inclination angle α lowers both mass and heat transfer efficiency while simultaneously building up the drag on the surface, as indicated by the skin friction coefficient. This observation reveals the ability of α to impede fluid motion and modulate transport phenomena. Furthermore, an increased slip velocity λ near the wall improves heat transmission and surface friction. Yet, this enhancement is accompanied by a decline in mass transfer rates. This suggests that although λ stimulates surface interactions, it restricts the bulk particle mobility.

Table 1 Computational results for $-f''(0)$, $-\xi'(0)$ and $-\theta'(0)$ across numerous values of λ , α and β , when $Ec = K = 0.1$, $N_b = N_t = 0.3$, $Le = 5$, $Pr = 6.8$ and $M = n = 2$.

α	β	$-\xi'(0)$		$-f''(0)$		$-\theta'(0)$	
		$\lambda = 0.1$	$\lambda = 0.3$	$\lambda = 0.1$	$\lambda = 0.3$	$\lambda = 0.1$	$\lambda = 0.3$
30°	0.1	1.203328	1.237992	1.226289	1.113796	1.676442	1.659818
45°	0.1	1.193411	1.227790	1.373090	1.247130	1.670801	1.654266
60°	0.1	1.184905	1.219039	1.474533	1.339267	1.664411	1.647939
30°	0.2	1.064892	1.095569	1.226289	1.113796	1.470562	1.456011
45°	0.2	1.056116	1.086540	1.373090	1.247130	1.465614	1.451111
60°	0.2	1.048589	1.078796	1.474533	1.339267	1.460009	1.445561
30°	0.3	0.845153	0.869498	1.226289	1.113796	1.284334	1.267339
45°	0.3	0.838188	0.862333	1.373090	1.247130	1.280012	1.267339
60°	0.3	0.832214	0.856187	1.474533	1.339267	1.275117	1.262492

3.1 Validation of the Code

To validate the precision of our findings, a comparison was conducted with previously published results by Dodda et al. [23], albeit with certain limitations in their models ($\alpha = 90^\circ$ and $K = 0$). A quantitative comparison of the $-f''(0)$, $-\xi'(0)$ & $-\theta'(0)$ across different values of λ and β in Table 2 confirms the consistency of our results.

Table 2 Comparative analysis for $-f''(0)$, $-\xi'(0)$ and $-\theta'(0)$ across numerous values of λ and β , when $\alpha = 90^\circ$, $K = 0$, $M = 1$, $N_b = N_t = 0.3$, $Le = 2$, $Pr = 5$. and $Ec = 0.1$

β	λ	$-\xi'(0)$		$-f''(0)$		$-\theta'(0)$	
		Dodda et al. [23]	Present Results	Dodda et al. [23]	Present Results	Dodda et al. [23]	Present Results
0.1	0.3	0.919926	0.919930	1.070591	1.070591	1.940784	1.940785
0.1	0.5	0.963265	0.963268	0.897480	0.897478	1.904185	1.904187
0.5	0.1	0.208106	0.208109	1.319597	1.319596	1.219905	1.219903
0.3	0.1	0.447819	0.447821	1.319597	1.319596	1.502959	1.502959

4. Conclusions

This work addresses the influence of nanofluid’s magnetohydrodynamic boundary layer flow across a non-linear inclined stretched surface situated in a porous material. It takes into account the affects of velocity and thermal slip conditions. Numerical computations were obtained by employing the FDKBI approach. The subtle findings from this research emphasize the complex relationships among these variables and their significance in determining flow patterns. A complete study of these variables reveals their combined and separate effects on the profiles of temperature, concentration, and velocity. Significant results from this research are:

1. Higher inclination angles enhance both concentration and temperature, while simultaneously diminishing the velocity profile.
2. An increase in permeability enhances fluid mobility by lowering flow resistance, leading to higher thermal conductivity, faster flow and a thinner velocity boundary layer. while, concentration decreases initially closer to the surface but rises further away.
3. Both concentration and temperature trajectories demonstrate a pronounced upward trend with increasing magnetic field strength, while fluid velocity experiences a decline.
4. Slip velocity improves heat transmission of the nanofluid.

ABBREVIATIONS	
B_0	Uniform magnetic field strength
$B(x)$	Variable magnetic field strength
a	Stretching rate
C	Nanofluid concentration
n	Non-linear stretching factor
C_f	Skin-friction
N_b	Brownian motion parameter

C_p	Nanoparticle specific heat
C_∞	Concentration of the free stream
C_w	Concentration of the stretching sheet
D_r	Thermophoresis diffusion Coefficient
N_t	Diffusion coefficient of thermophoresis
D_m	Brownian diffusion Coefficient
$f(\eta)$	Dimensionless stream function
Ec	Eckert number
$-f''(0)$	Skin friction coefficient
D_0	Initial thermal slip
g	Acceleration due to gravity
$f'(\eta)$	Non dimensional velocity
M	Magnetic parameter
Gr_x	Local Grashof number
N_0	Initial velocity slip
Gc_x	Local modified Grashof number
Pr	Prandtl number
K_d	Dimensional permeability parameter
K	Non-dimensional permeability parameter
Nu	Nusselt number
Sh	Sherwood number
u	Velocity component parallel to the x direction
T	Dimensional temperature of the nanofluid
Re	Reynolds number
T_∞	Free stream temperature
x, y	Cartesian coordinate axis
T_w	Surface temperature
v	Velocity component parallel to the y direction
D	Thermal slip factor
u_w	Stretching sheet velocity
Greek Letters	
η	Non-dimensional similarity variable
κ_s	Nanoparticles thermal conductivity
β_T	Thermal expansion coefficient
β_C	Concentration expansion coefficient
α	Inclination parameter

$\xi(\eta)$	Non-dimensional concentration
κ_{nf}	Nanofluid thermal conductivity
κ_f	Base fluid thermal conductivity
$\theta(\eta)$	Non-dimensional temperature
σ	Electric conductivity
ϕ	Nanoparticles solid volume fraction
α_{nf}	Nano fluid thermal diffusivity
τ_w	Wall shear stress
ν_f	Base fluid kinematic viscosity
μ_{nf}	Nano fluid viscosity
μ_f	Base fluid viscosity
ρ_{nf}	Nano fluid density
ρ_f	Base fluid density
$(\rho C_p)_{nf}$	Nano fluid heat capacitance
ρ_s	Nanoparticles density
$(\rho C_p)_f$	Base fluid heat capacitance
$-\theta'(0)$	Local Nusselt number
$(\rho C_p)_s$	Nanoparticles heat capacitance
ψ	Stream function
$-\xi'(0)$	Local Sherwood number

Conflict of Interest: The authors declare no conflicts of interest.

Data Availability: Data will be made available on reasonable request.

References

[1] Jamrus, F. N., Waini, I., Khan, U., & Ishak, A. (2024). Effects of magnetohydrodynamics and velocity slip on mixed convective flow of thermally stratified ternary hybrid nanofluid over a stretching/shrinking sheet. *Case Studies in Thermal Engineering*, 55, 104161. <https://doi.org/10.1016/j.csite.2024.104161>

[2] Bansal, S., Kumar, A., Pal, J., Goyal, I., & Negi, A. S. (2024). Influence of Thermal Wall and Velocity Slips on Non-Darcy MHD Boundary Layer Flow of a Nanofluid over a Non-linear Stretching Sheet. *Journal of Physics: Conference Series*, 2844, 012018. <https://doi.org/10.1088/1742-6596/2844/1/012018>

[3] Abbas, W., Megahed, A. M., Ibrahim, M. A., & Said, A. A. M. (2023). Non-Newtonian Slippery Nanofluid Flow Due to a Stretching Sheet Through a Porous Medium with Heat Generation and Thermal Slip. *Journal of Nonlinear Mathematical Physics*, 30(3), 1221–1238. <https://doi.org/10.1007/s44198-023-00125-5>

- [4] Krishna, M. V., & Chamkha, A. J. (2019). Hall and ion slip effects on MHD rotating boundary layer flow of nanofluid past an infinite vertical plate embedded in a porous medium. *Results in Physics*, 15, 102652. <https://doi.org/10.1016/j.rinp.2019.102652>
- [5] Hayat, T., Shafiq, A., Alsaedi, A., & Shahzad, S. A. (2016). Unsteady MHD flow over exponentially stretching sheet with slip conditions. *Applied Mathematics and Mechanics*, 37(2), 193–208. <https://doi.org/10.1007/s10483-016-2024-8>
- [6] Reddy, Y. D., & Goud, B. S. (2023). Comprehensive analysis of thermal radiation impact on an unsteady MHD nanofluid flow across an infinite vertical flat plate with ramped temperature with heat consumption. *Results in Engineering*, 17, 100796. <https://doi.org/10.1016/j.rineng.2022.100796>
- [7] Kumar, B., & Padmaja, K. (2022). Buoyancy and Ohmic Heating Effects on MHD Nanofluid Flow over a Vertical Plate Embedded in a Porous Medium. *Journal of Porous Media*, 25(8), 1-18. <https://doi.org/10.1615/JPorMedia.2022041707>
- [8] Goud, B. S., Srilatha, P., Mahendar, D., Srinivasulu, T. & Reddy, Y. D. (2024). Thermal radiation effect on thermostatically stratified MHD fluid flow through an accelerated vertical porous plate with viscous dissipation impact. *Partial Differential Equations in Applied Mathematics*, 7, 100488. <https://doi.org/10.1016/j.padiff.2023.100488>
- [9] Bulatova, R. R., Samokhin, V. N., & Chechkin, G. A. (2020). Equations of Symmetric MHD-Boundary Layer of Viscous Fluid with Ladyzhenskaya Rheology Law. *Journal of Mathematical Sciences*, 244(2), 158–169. <https://doi.org/10.1007/s10958-019-04611-4>
- [10] Sudarmozhi, K., Iranian, D., & Al-Mdallal, Q. M. (2024). Revolutionizing energy flow: Unleashing the influence of MHD in the presence of free convective heat transfer with radiation. *International Journal of Thermofluids*, 22, 100662. <https://doi.org/10.1016/j.ijft.2024.100662>
- [11] Kakac, S., & Pramuanjaroenkij, A. (2009). Review of convective heat transfer enhancement with nanofluids. *International Journal of Heat and Mass Transfer*, 52(13), 3187–3196. <https://doi.org/10.1016/j.ijheatmasstransfer.2009.02.006>
- [12] Hyder, A., Lim, Y. J., Khan, I., & Shafie, S. (2024). Investigating Heat Transfer Characteristics in Nanofluid and Hybrid Nanofluid Across Melting Stretching/Shrinking Boundaries. *Bio Nano Science*, 14(2), 1181–1195. <https://doi.org/10.1007/s12668-024-01309-z>
- [13] Ouada, M., Kezzar, M., Talbi, N., Eid, M. R., Sari, M. R., Yousef, W. M., & Elsaid, E. M. (2023). Heat transfer characteristics of moving longitudinal porous fin wetted with ternary (Cu, Al₂O₃, TiO₂) hybrid nanofluid: ADM solution. *The European Physical Journal Plus*, 138(9), 861. <https://doi.org/10.1140/epjp/s13360-023-04459-3>
- [14] Seid, E., Haile, E., & Walelign, T. (2022). Multiple slip, Soret and Dufour effects in fluid flow near a vertical stretching sheet in the presence of magnetic nanoparticles. In *International Journal of Thermofluids*, 13, 100136. <https://doi.org/10.1016/j.ijft.2022.100136>
- [15] Kaviany, M. (2012). *Principles of Heat Transfer in Porous Media*. Springer. <https://doi.org/10.1007/978-1-4684-0412-8>
- [16] Chernukha, O. Y., & Bilushchak, Y. (2024). Mathematical Modeling of the Processes of Convective Diffusion and Sorption in a Three-Layer Porous Body. I. Mass Transfer of Impurity Particles with a Porous Solution. *Journal of Mathematical Sciences*, 279(2), 247–259. <https://doi.org/10.1007/s10958-024-07008-0>
- [17] Zhang, X., Yang, D., Israr Ur Rehman, M., & Hamid, A. (2021). Heat Transport Phenomena for the Darcy–Forchheimer Flow of Casson Fluid over Stretching Sheets with Electro-Osmosis Forces and Newtonian Heating. *Mathematics*, 9(19), 2525. <https://doi.org/10.3390/math9192525>

- [18] Bansal, S., Pal, J., Bisht, M. S., & Fartyal, P. (2024). Influence of Nanofluids on Boundary Layer Flow over an Inclined Stretching Sheet in a Porous Media along with Magnetic Field. *International Journal of Mathematical, Engineering and Management Science*, 9(2), 267–282. <https://doi.org/10.33889/IJMEMS.2024.9.2.014>
- [19] Gupta, R. S. (2015). *Elements of Numerical Analysis*. Cambridge University Press. <https://doi.org/10.1017/CBO9781316212516>
- [20] Smith, G. D. (1985). *Numerical Solution of Partial Differential Equations: Finite Difference Methods*. Oxford University Press.
- [21] Sarif, N. M., Salleh, M. Z., & Nazar, R. (2013). Numerical Solution of Flow and Heat Transfer over a Stretching Sheet with Newtonian Heating using the Keller Box Method. *Procedia Engineering*, 53, 542–554. <https://doi.org/10.1016/j.proeng.2013.02.070>
- [22] Rafique, K., Alqahtani, A. M., Ahmad, S., Aslam, S., Khan, I., & Singh, A. (2024). Numerical simulations of Williamson fluid containing hybrid nanoparticles via Keller box technique. *Discover Applied Sciences*, 6(3), 80. <https://doi.org/10.1007/s42452-024-05729-0>
- [23] Dodda Ramya, Raju, R. S., Rao, J. A., & Chamkha, A. J. (2018). Effects of velocity and thermal wall slip on magnetohydrodynamics (MHD) boundary layer viscous flow and heat transfer of a nanofluid over a nonlinearly-stretching sheet: A Numerical Study. *Propulsion and Power Research*, 7(2), 182–195. <https://doi.org/10.1016/j.jprr.2018.04.003>
- [24] Ishak, A., Jafar, K., Nazar, R., & Pop, I. (2009). MHD stagnation point flow towards a stretching sheet. *Physica A: Statistical Mechanics and Its Applications*, 388(17), 3377–3383. <https://doi.org/10.1016/j.physa.2009.05.026>
- [25] Brinkman, H. C. (1952). The viscosity of concentrated suspensions and solutions. *The Journal of Chemical Physics*, 20(4), 571–581. <https://doi.org/10.1063/1.1700493>
- [26] James Clerk Maxwell. (1954). *A treatise on electricity and magnetism*. Dover Publications, Inc.
- [27] Keller, H. B., & Cebeci, T. (1972). Accurate numerical methods for boundary-layer flows. ii: Two dimensional turbulent flows. *AIAA Journal*, 10(9), 1193–1199. <https://doi.org/10.2514/3.50349>
- [28] Ishak, A., Nazar, R., & Pop, I. (2008). Uniform suction/blowing effect on flow and heat transfer due to a stretching cylinder. *Applied Mathematical Modelling*, 32(10), 2059–2066. <https://doi.org/10.1016/j.apm.2007.06.036>
- [29] Xuan, Y., Li, Q., & Hu, W. (2003). Aggregation structure and thermal conductivity of nanofluids. *AIChE Journal*, 49, 1038–1043. <https://doi.org/10.1002/aic.690490420>